Solar Energy Materials and Solar Cells 174 (2018) 65–76

Contents lists available at ScienceDirect

Solar Energy Materials and Solar Cells

journal homepage: www.elsevier.com/locate/solmat

Nanometre-scale optical property fluctuations in Cu_2ZnSnS_4 revealed by low temperature cathodoluminescence

B.G. Mendis[a,*], A.A. Taylor[a,b,1], M. Guennou[c], D.M. Berg[d,2], M. Arasimowicz[d], S. Ahmed[e], H. Deligianni[e], P.J. Dale[d]

[a] Dept. of Physics, Durham University, South Road, Durham DH1 3LE, UK
[b] EMPA, Laboratory for Mechanics and Nanostructures, Feurwerkerstrasse 39, CH-3602 Thun, Switzerland
[c] Luxembourg Institute of Science and Technology, Materials Research and Technology Department, 41 rue du Brill, 4422 Belvaux, Luxembourg
[d] Physics and Materials Science Research Unit, Université du Luxembourg, 41 rue du Brill, L-4422 Belvaux, Luxembourg
[e] IBM, Thomas J. Watson Research Center, 1101 Kitchawan Road, Yorktown Heights, NY 10598, USA

ARTICLE INFO

Keywords:
Optical properties
Order-disorder
Band tailing
Cu2ZnSnS4
Cathodoluminescence

ABSTRACT

Band tailing is a major contributing factor to the large open circuit voltage (V_{oc}) deficit that is currently limiting Cu_2ZnSnS_4 (CZTS) photovoltaic devices. It occurs in highly doped, highly compensated semiconductors and gives rise to a non-uniform electronic band structure. Here we report spatially resolved fluctuations in CZTS optical properties using low temperature cathodoluminescence (CL) in a scanning electron microscope (SEM). Principal component analysis reveals three CL peaks whose relative intensity vary across domains ~ 100 nm in size. It is not known whether the non-uniform optical properties are due to changes in composition or due to structural order-disorder at constant composition. Measurement of composition with energy dispersive X-ray (EDX) analysis in an SEM and ordering with Micro-Raman mapping revealed CZTS to be uniform within the spatial resolution (estimated at ~ 0.4 μm and 1.1 μm respectively) and sensitivity of the two techniques. The CL results are consistent with the presence of band tailing in CZTS.

1. Introduction

Cu_2ZnSnS_4 (CZTS) contains only earth abundant, non-toxic elements and is the leading absorber layer material for Tera Watt solar electricity generation [1]. The open circuit voltage (V_{OC}) deficit is however large compared to the structurally similar $Cu(In,Ga)Se_2$ (CIGS) photovoltaic devices [2,3], and is the main reason for a relatively modest record cell efficiency of 12.6% for the S, Se variant $Cu_2ZnSn(S,Se)_4$ or CZTSSe [4]. A key difference between CZTS and CIGS is the extensive band tailing in the former [3,5]. Band tailing in CZTS is related to: (i) Urbach tails in absorption and quantum efficiency spectra [5], (ii) broadening of Raman vibration modes [6,7], (iii) S-shaped temperature dependence of the photoluminescence peak [8,9] and (iv) an anomalously long carrier lifetime at low temperature [3,10]. Band tailing is common in highly doped, highly compensated semiconductors and is due to statistical fluctuations in the local dopant (i.e. donor and acceptor) concentration. This results in a spatially varying band structure with electron and hole potential wells [11], as illustrated in Fig. 1. Electronic states are present within the band gap and the mobility of carriers within these tail states is smaller than 'free' (i.e. un-trapped) carriers. The lower overall mobility could therefore be a contributing factor to the short carrier diffusion length [2] and hence limited efficiency of CZTS.

Band tailing is due to band gap and/or electrostatic potential fluctuations. The former can be induced by ordering or, in the case of CZTSSe, variations in the anion and/or cation concentrations. On the other hand point defects in the form of vacancies and anti-site atoms can act as either donors or acceptors. Variations in dopant (i.e. donor and acceptor) concentration gives rise to electrostatic potential fluctuations. The low formation energy defects are typically anti-site atoms of Cu and Zn, such as the Cu_{Zn} acceptor or neutral [Cu_{Zn} + Zn_{Cu}] defect complex [12]. Neutron diffraction has revealed significant inter-mixing of Cu and Zn in the Wyckoff 2*c* and 2*d* positions of the kesterite phase (space group $I\bar{4}$; [13]). Even for relatively slow sample cooling rates of 1 K/h the Cu, Zn disorder can be as high as 30% [13]. Furthermore, chemical analysis in a scanning transmission electron microscope (STEM) has detected Zn_{Cu} donor clusters smaller than 5 nm in size [14], as well as ~ 20 nm size domains where Cu substitutes for either Zn or

* Corresponding author.
E-mail address: b.g.mendis@durham.ac.uk (B.G. Mendis).
[1] Now at: Materials Department, University of California, Santa Barbara, CA 93106, USA.
[2] Now at: Delaware State University, 1200 North DuPont Highway, Dover, DE 19901, USA.

http://dx.doi.org/10.1016/j.solmat.2017.08.028
Received 24 March 2017; Received in revised form 15 August 2017; Accepted 20 August 2017
Available online 31 August 2017

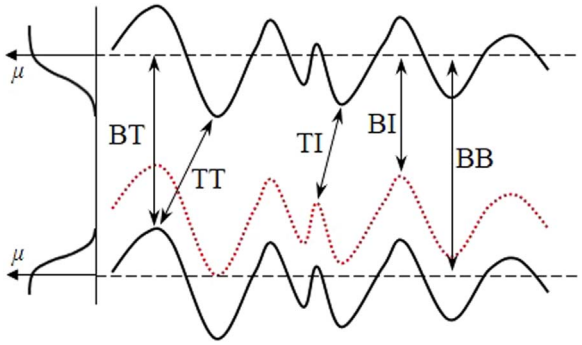

Fig. 1. Conduction and valence band edge diagram for a heavily doped, *p*-type semiconductor. The red dotted line is the acceptor energy level. Carrier mobility (μ) at the band edges and recombination pathways are also indicated. These include 'BT' (band to tail), 'TT' (tail to tail), 'TI' (tail to impurity), 'BI' (band to impurity) and 'BB' (band to band) recombination. (For interpretation of the references to color in this figure legend, the reader is referred to the web version of this article.)

Sn [15]. In the former case the local doping concentration, estimated at 10^{22} cm^{-3} [14], was high enough to render the semiconductor degenerate, while for the latter the amplitude of the composition fluctuation was estimated to be less than 1 at% or equivalently ~ 10^{20} cm^{-3} [15].

The optical properties of CZTS have thus far largely been measured on the material as a whole, with less emphasis on uncovering any fluctuations within the material itself. Barragan et al. [16] have reported a spatially non-uniform micro-Raman signal, but this was due to the presence of secondary phases such as ZnS, rather than an intrinsic property of the CZTS itself. In this paper we present evidence for spatially non-uniform optical properties in CZTS using cathodoluminescence (CL) in a scanning electron microscope (SEM). Photoluminescence spectra measured from bulk CZTS typically show a broad featureless peak [9], which makes it difficult to extract the underlying recombination pathways. The high spatial resolution in an SEM however provides more local information and by cooling the specimen close to liquid-He temperature the effect of phonon broadening of the luminescence peaks can also be reduced. It is shown that the optical properties of CZTS can fluctuate over domains ~ 100 nm in size. The results complement previous findings on composition fluctuations in CZTS [14,15] and are consistent with the observation of band tailing in this material.

2. Experimental methods

The sample precursor consisted of electrodeposited Cu/Sn/Zn layers [17] which were then sulphurised by annealing in a mixed S, SnS atmosphere [18] by placing 100 mg of S and 20 mg of SnS powder in a graphite box with an internal volume of 20 cm^3. The annealing procedure consisted of two steps: (i) a fast temperature ramp to 100 °C at which the sample remained for 1 h at pressures of less than 1 Pa of forming gas (10% H_2 in N_2) and (ii) a fast temperature ramp to temperatures of around 550 °C at which the sample was annealed for 2 h in a 50 kPa atmosphere of forming gas. During the second annealing step the atmosphere inside the tube furnace further contained gaseous sulphur and tin-sulphide molecules at an undetermined partial pressure which originated from elemental sulphur and tin-sulphide pellets that were placed inside the furnace together with the samples at the beginning of the annealing procedure. After the second reaction step the samples were physically removed from the hot zone in order to quickly cool down the samples and abruptly stop any reaction.

Complete solar cell devices were made by chemically depositing a ~ 50 nm layer of CdS, followed by sputtering 80 nm of i-ZnO and 400 nm of Al:ZnO, and by e-beam evaporation of front contacts made from Ni then Al. Current density-voltage (JV) measurements on completed devices were made with a home built setup, using a Keithly 2400 series source meter in a four wire kelvin probe configuration with 120 V ELH halogen lamp illumination calibrated with a certified mono crystalline silicon solar cell to give an output of 1000 W m^{-2} at 25 °C. The kesterite devices were kept at 25 °C using a peltier plate. The reference cell was certified under AM1.5 G illumination by the Fraunhofer ISE, Germany.

External quantum efficiency (EQE) measurements were made in a homemade system. White light passes through a Bentham TMC300 monochromator with 5 nm resolution to produce monochromatic light. The light is collimated and chopped with a Scitec instruments optical chopper with an output frequency of 133 Hz. The system is calibrated with Si and InGaAs photodiodes which were certified by the Physikalisch-Technische Bundesanstalt (German national standards laboratory). The photodiodes and kesterite cells were measured without bias using a homebuilt potentiostat acting as a current amplifier connected to an SR850 lock-in from Stanford Research Systems. The optical chopper outputs its frequency modulation to the lock-in for synchronisation. Both JV and EQE measurements were made after annealing the devices on a hot plate with surface temperature of 200 °C for 60 s in air.

For electron microscopy a ~ 2×1 mm area of the sample was ultrasonically cut and mechanically polished using 0.1 μm grade diamond paper followed by low energy argon ion-polishing in a Gatan PIPS machine. This particular sample was not a completed device and had the front surface of the CZTS absorber layer exposed for electron microscopy analysis. A Hitachi SU-70 SEM at Durham was used for room temperature CL measurements of the ZnS secondary phases (Section 3.2) as well as energy dispersive X-ray (EDX) analysis to determine the composition uniformity of CZTS. The operating voltage was 15 kV. A Tescan Lyra 3 dual-beam SEM at EMPA was used for EDX area mapping of the ZnS precipitates at 15 kV. Nano-indents were placed on the sample surface to act as fiducial markers, so that approximately the same area could be used for analysis between different microscopes. Cross-section images were obtained using a 3 kV electron beam in an FEI Helios 600 focussed ion-beam (FIB) microscope at Durham. Prior to milling a platinum protective layer was deposited on the specimen surface in order to protect the underlying structure from ion-beam damage. Rough milling of the trench was carried out at 30 kV ion-beam voltage, while the cross-section was polished at 16 kV. The CL data on CZTS (Section 3.3) was obtained using a prototype Attolight SEM operating at 5 kV beam voltage, with the sample liquid-Helium cooled to 10 K. Unfortunately the Attolight results preceded the other electron microscopy work in this paper and therefore it is unlikely the data was acquired from the same area of the sample. Nevertheless it should be noted that the overall microstructure did not vary between different regions of the sample. Attolight CL data was processed using principal component analysis, implemented via the 'Cornell Spectrum Imager' freeware package [19].

Micro-Raman mapping was also performed on the same area of the sample, which was located by finding the nano-indents under an optical microscope. A Renishaw inVia micro-Raman spectrometer was used for ZnS and CZTS mapping in two different configurations. For UV spectra, the 325 nm line of a He-Cd laser was used at ~ 0.8 mW power, focussed onto the sample with a microscope objective ×40 with 0.5 numerical aperture (NA), in combination with a 2400 lines/mm grating, the spot size and spectral resolution being 0.8 μm and 3.5 cm^{-1} respectively. For the near-IR spectra, the excitation wavelength was 785 nm, laser power ~ 0.5 mW, the grating 1200 lines/mm, the microscope objective ×100 with 0.9 NA, giving a spot size and spectral resolution of 1.1 μm and 1.3 cm^{-1} respectively. The maps were acquired over a 20 × 20 μm^2 square with 1 μm step size. Principal component analysis was used to smooth the Raman spectra.